The role of dynamic measurements in characterizing the mechanical behaviour of a high porosity rock

T. Rotonda

University of Rome *La Sapienza*, Italy

ABSTRACT: In this paper some results from laboratory tests on a clastic rock (calcarenite) having a porosity of 0.3 are illustrated and discussed. The mechanical behaviour of the calcarenite has been investigated through measurements of its textural characteristics and of the seismic wave velocities in both dry and saturated conditions on unstressed specimens. To study the mechanical behaviour of the rock during loading, uniaxial and triaxial tests have been carried out; the static measurements have been supplemented by dynamic measurements of the P- and S-wave velocities in the direction of the applied load and in the transversal direction for the uniaxial compression tests. The results of the measurements have outlined that porosity alone is insufficient in evaluating the elastic properties of the rock, while it is important to gain a thorough understanding of its textural characteristic, which can determine a composite distribution of water inside the voids and large differences in the elastic moduli. Wave velocities and also wave amplitudes have been found to be a very sensitive index of textural variations.

1 INTRODUCTION

Investigation methods based on dynamic measurements, that are essentially measurements of the velocity of seismic waves, are currently utilized by researchers for the textural characterization of rock materials and for evaluating the elastic parameters of rocks in different stress and strain conditions. Experimental studies on the dynamic characteristics of soft clastic rocks have been recently carried out by Zamora & Poirier 1990, Sayers et al. 1990, Scott et al. 1993, Hilbert et al. 1994, Berge et al. 1995. The study of these rocks has been prompted also by researchers working in the field of hydrocarbons production (Bourbie & Zinszner 1985, Papamichos et al. 1997); these studies are often accompained by experimental tests on the transport properties of the rocks (e.g. permeability or resistivity).

Within this framework it has been deemed interesting to study the behaviour of calcarenites, which are widely present in the South of Italy and whose mechanical characteristics are important for engineering applications.

This paper examines the behaviour of a calcarenite from Sicily (Italy), where a cavern for a storage hydroelectric plant was built at a depth of about 350 m during the 1980s. A series of investigations including field and laboratory measurements were conducted in the area and some of the results were presented by Borsetto et al. (1984). We have reanalyzed these data and, in order to obtain further information about the mechanical behaviour of the calcarenite, we decided to carry out new experimental tests in the laboratory. In particular, a more thorough understanding of the mechanical behaviour of the calcarenite was obtained through measurements of the textural characteristics and of the seismic wave velocities, both in unstressed conditions and during loading tests.

The data obtained in the investigations of the 1980s are interesting for the widely varying mechanical characteristics they provide of the tested specimens, due in large measure to the variability of porosity (0.05 to 0.42). The new tests recently performed and discussed in the following have focussed on the lithotype inside which the cavern was excavated, whose porosity was found to be in the range 0.28-0.32 (volumic mass 1.8-2.0 Mg/m^3).

2 PHYSICAL PROPERTIES OF THE TESTED ROCK

2.1 *Optical microscope analysis*

The rock is a fine to medium-grained biocalcarenite of Miocene age, called *Palazzolo formation*. Calcite is the most abundant mineral (98%).

Figure 1 shows the texture of the rock, as it appears through thin sections viewed under the optical microscope. Fossils, of different types and sizes, are

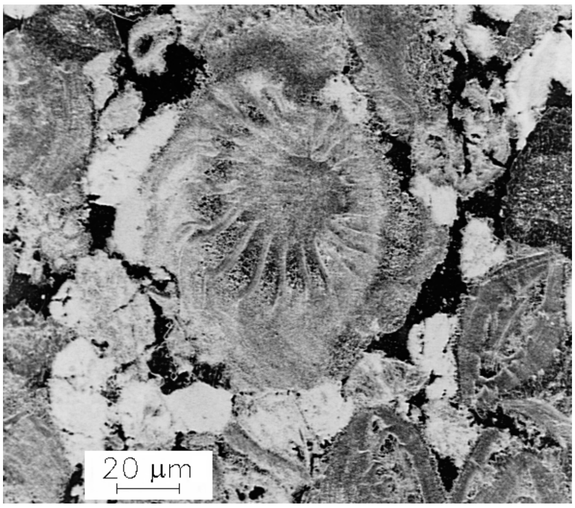

Figure 1. Thin section at the optical microscope showing fossils. Voids are in black.

very abundant and most of them are intact; the characteristic dimension is 40-100 µm. The cement is mostly constituted by isometric calcite grains with a typical dimension of 15-20 µm; the contact points between the various constituents are rare.

Porosity, which is characterized by a wide distribution of dimensions, results from intergranular voids, having irregular shape, and from very small, usually rounded, pores inside the fossils. Some of the intergranular pores were produced by the chemical dissolution of pre-existing grains.

The optical examination indicates that the sedimentation process occurred slowly, so as to leave the fossils almost entirely intact, and that lithification occurred early in the sedimentation process itself so as to originate a highly porous rock, whose strength was high enough to bear the lithostatic stress.

2.2 *Density and porosity*

For the mechanical investigation 35 cylindrical specimens (54 mm in diameter and with a height-to-diameter ratio of 2) were prepared. In order to determine dry density, geometrically regular specimens were dried up to a constant weight under vacuum; heating them in an oven was avoided because calcite is known to be sensitive to thermal microfissuring. A mean value of the density of 1.90 Mg/m^3 was derived from these measurements.

Solid matrix density has been determined on finely grounded materials with a helium picnometer, obtaining an average value of 2.715 Mg/m^3. From a comparison between the densities of the solid matrix and that of the dry specimens a mean value of 0.301 of the total porosity ϕ_t was determined.

Pore connectivity has been evaluated from the water content of saturated specimens. Saturation can be related to total porosity ϕ_t, connected porosity ϕ_c or free porosity ϕ_f; the latter can be defined as the porosity saturated by a wetting fluid (water) in the presence of a non wetting fluid (e.g. air). The related degrees of saturation will be indicated respectively by S_t, S_c, and S_f.

Full saturation of connected voids was obtained by vacuum drying the specimens in a desicator and by subsequently introducing deaerated water. The amount of isolated porosity was found to be very small with respect to connected porosity ϕ_c (0.025 against 0.276); but this value could be slightly underestimated if closed pores had happened to be present in the material utilized in the helium picnometer.

Saturation of free porosity was obtained by immerging the specimens in water for a very long time up to a seemingly constant weight, obtaining values of S_t of about 0.70.

Additional information about the porosity structure has been obtained by means of mercury porosimeter tests on two samples (Fig. 2). The superimposition of three distinct pore throat distributions can be identified: they have mean values of 7, 2 and 0.3 µm, which correspond to a partial porosity of about 0.085, 0.050 and 0.155 respectively. The measured porosity (reached at the maximum pressure of 200 MPa) is about 0.290, which is in good agreement with the measurements made on the cylindrical specimens. The two larger characteristic dimensions possibly correspond to the intergranular voids and to the pores inside the fossils, which have been observed in thin sections. The very small voids will not show up in thin sections and they could be partly ascribed to microcracks, possibly at the grain contacts; the strong connectivity detected for voids of this size is quite surprising.

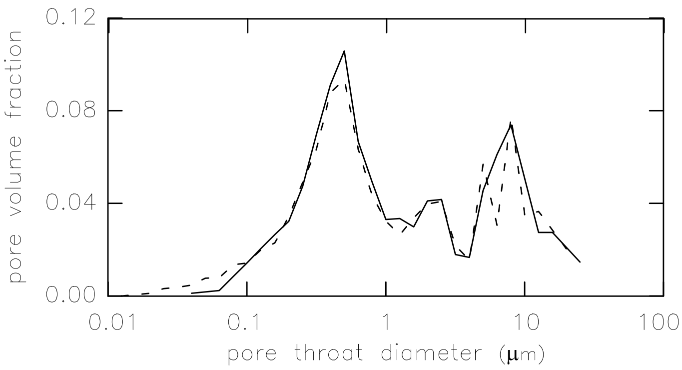

Figure 2. Pore throat size distributions from two samples of the *Palazzolo limestone*, obtained from mercury intrusion porosimetry tests.

3 DYNAMIC PROPERTIES IN UNSTRESSED CONDITIONS

Ultrasonic velocities of longitudinal (P) and shear (S) waves have been determined on cylindrical specimens by measuring the transit time of a square wave. The impulse was generated by the Pundit pulser (Wu et al. 1991) through Panametrics piezoelectric transducers (15 mm in diameter), having a

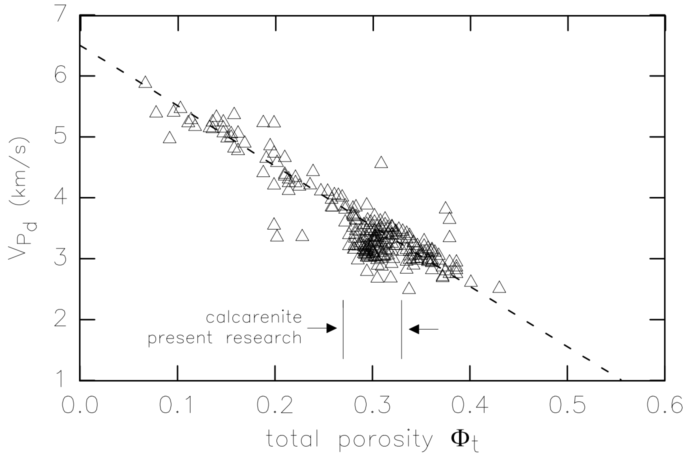

Figure 3. P-wave velocity obtained from dry specimens vs. total porosity. Data from Borsetto et al. 1994 are included.

typical frequency of 1 MHz. A Tektronix TDS 420 digital storage oscilloscope (maximum digitazing rate of 100 MHz) was utilized to acquire waveforms. Coupling of the transducers with the ends of the specimens was obtained by means of a slight load (50 kN), avoiding the use of an acoustic couplant.

3.1 *Dry conditions*

Figure 3 shows the P-wave velocity determined on dry specimens as a function of total porosity; the data available from Borsetto et al. (1984) are also included because they cover a wider range of porosities (0.05-0.42). An almost linear trend between velocity and porosity (standard deviation of estimate is 0.16 km/s) is observed, with an intercept on the porosity axis at about 0.65. A similar linear variation was observed in other clastic formations in which porosity varied up to approximately 0.30 (Bourbie & Zinszner 1985, Han et al. 1986, Blangy et al. 1993).

Also the shear wave velocity (not shown) measured on the calcarenite presents a correlation with porosity, but slighter than longitudinal velocity.

3.2 *Saturated conditions*

Measurements of the P- and S-wave velocities have been carried out also in different saturation conditions.

Full saturation of connected porosity ($S_c = 1.00$) causes an increase in the P-wave velocity, with respect to dry specimens (Fig. 4), while S-wave values do not show a significant variation. The saturation condition of free porosity ($S_f = 1.00$) produces lower values of P-wave velocity with respect to the dry values (Fig. 4) (no data are available for the shear wave).

These behaviours can be compared with the results of in situ seismic velocity determinations performed during the 1980s; as the water table was

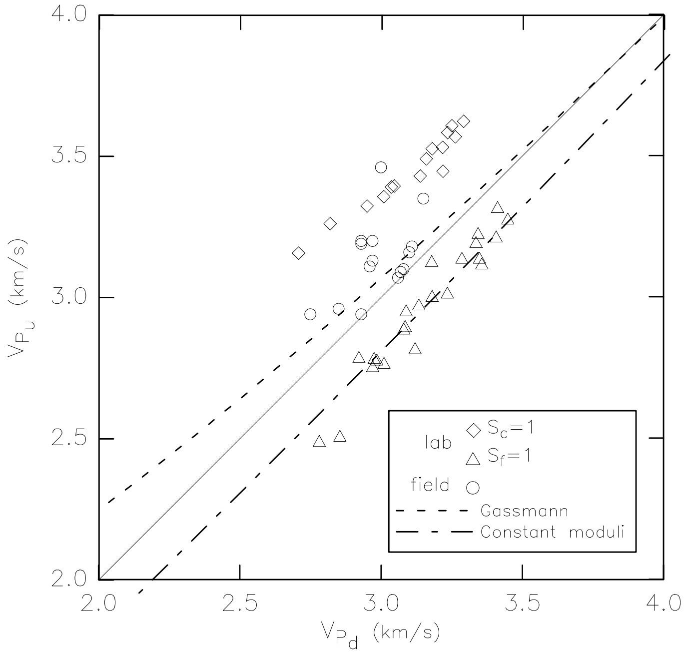

Figure 4. Correlation of P-wave velocities in dry and saturated conditions determined in laboratory and in situ. Also curves from the theoretical models are displayed (see text).

located at the midheight of one of the exploratory tunnels, it was possible to measure the P-wave velocities in the same material both above and underneath the water table. The P-wave velocity (Fig. 4) was found to be higher underneath the water table, but not as much as found in the laboratory tests.

For a better appraisal of the influence of partially saturated conditions, the effect of immersion of an initially dry specimen (imbibition test) and the effect of drainage of an initially saturated specimen (drainage test) was investigated (Fig. 5). Starting from a fully saturated specimen, water drainage causes

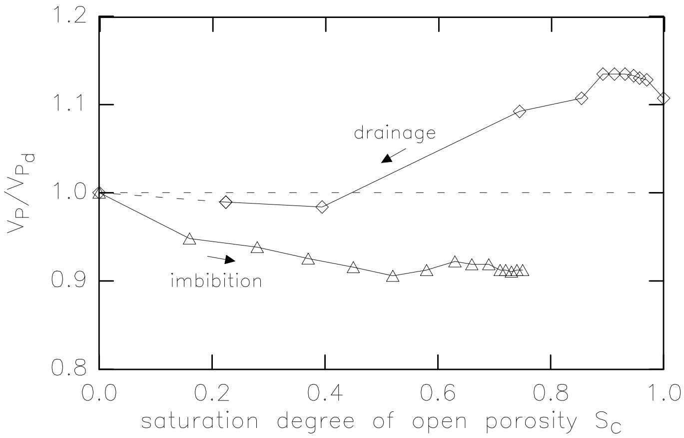

Figure 5. P-wave velocities (normalized with respect to dry velocity) measured for two specimens during a drainage and an imbibition test vs. the degree of saturation of the connected porosity. In the drainage test the completely dry condition was obtained under vacuum (dashed line). In the imbibition test only the free porosity was reached.

initially a slight increase in velocity; subsequently the P-wave velocity decreases progressively toward a minimum value. The specimen in equilibrium with the ambient conditions of the laboratory still contains some water and thus velocity is slightly lower than that observed in the fully dried specimen in a vacuum. This behaviour was attributed by Murphy (1984) to a weakening of the elastic frame in the presence of a small quantity of adsorbed water.

In the imbibition test, partial saturation causes a steady decrease in velocity, which reaches a constant value after a short time (less than 5 hours for a diameter of the specimen of 54 mm). Even when the specimen is immerged in water for a few months the air in the pores with the lower aspect ratio will not be replaced by water.

Similar differences between velocities during the drainage and imbibition tests were also observed in other clastic rocks, such as sandstone (Knight & Nolen-Hoeksema 1990).

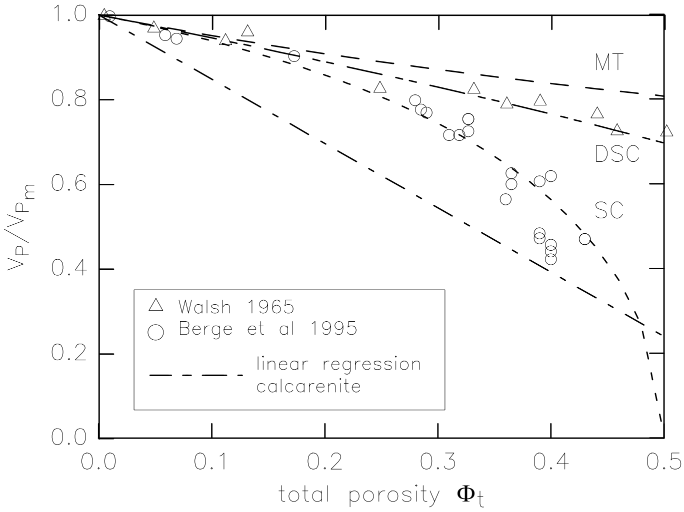

Figure 6. P-wave velocities (normalized with respect to the velocities of the related intact materials) vs. total porosity. Data derive from artificial clastic rocks; our data are represented by a linear regression curve (Fig. 3). Also curves from three theoretical models are displayed.

4 THEORETICAL MODELS

4.1 *Dry conditions*

It is interesting to compare the relationship between porosity and P-wave velocity observed in the *Palazzolo limestone* (Fig. 3) with the predictions of some theoretical models and with the results of experimental tests carried out on idealized models of porous rocks.

The simplest theoretical models which have been proposed to represent the elastic properties of a medium containing voids derive from two different approaches: i) *equivalent stress* models, such as the Mori-Tanaka model (MT) (Mori & Tanaka 1973); ii) *equivalent material* models, such as the self-consistent model (SC) (O'Connell & Budiansky 1974) or the differential self-consistent model (DSC) (Cleary et al. 1980, Zimmerman 1991).

In general, the compliance of the cracked material is the sum of two contributions which derive respectively from the compliances of the matrix and of the voids. In each of these models the contribution of the voids to compliance depends on their shape and spatial distribution. In particular, the effect of voids in which two of the dimensions prevail over the third (microcracks) is greater than the effect of isometrically-shaped voids (pores). For the same type of voids there are wide differences in the predictions offered by the various models, especially at high void concentrations.

According to the equivalent stress theory (Mori-Tanaka models), void interaction is taken into account by scaling over the factor (1-ϕ_t) the contribution of voids to compliance. Deformation moduli approach zero when porosity tends to 1, while velocities present a finite value.

Figure 6 shows the relationships between porosity and P-wave velocity proposed by the different models for materials containing spherical voids. It is to be noted that in this case the results of the MT model correspond to the upper Hashin-Shtrikman bound and also to the Kuster & Toksoz (1974) model.

The same Figure 6 shows the results of some tests carried out by Walsh (1965) on glass specimens containing varying proportions of isometric holes, up to a maximum porosity of 0.70 (foamy structure). The Figure also shows the results of tests performed on an artificial clastic rock constituted by glass spheres, with partial welding at their contact in loading conditions (Berge et al. 1995). It is to be noted that for the Walsh material the velocities of the P- and S-waves were calculated from the static constants of compressibility tests (see Berge et al. 1995), whereas for the assemblage of spheres they were directly measured in dry and saturated conditions.

It can be observed that the Walsh results are intermediate between the MT and DSC models, whereas the behaviour of the assemblage of spheres is in good agreement with the SC model, which estimates a porosity limit of 0.50. From the analysis of these results it is clear that the knowledge of porosity alone is insufficient in evaluating the elastic properties of the material and that its texture has a prevailing influence.

From the same Figure 6 it is evident that the linear trend of the calcarenite is located below the assemblage of the spheres and, as was to be expected on the basis of its texture, it is much closer to the Berge material, rather than to that of a foam material. However, for calcarenite the investigations on the porosity structure and the results of dynamic measurements on unstressed specimens indicate that the voids frame is complex, and that microcracks

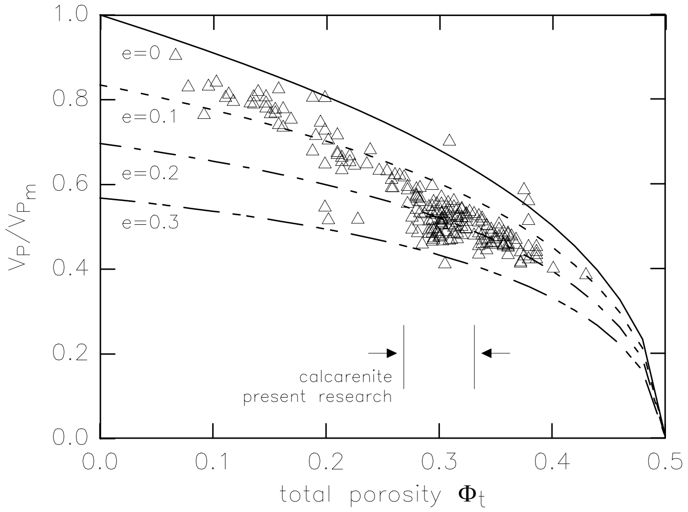

Figure 7. P-wave velocities (normalized with respect to the velocity of intact material V_{Pm}=6.5 km/s) vs. total porosity. The displayed curves derive from the SC model (K=77.7 GPa, ν=0.34) and are relative to materials with different crack densities (e=0.0÷0.3).

may be present.

For a material which contains randomly distributed cracks, the theoretical models indicate that the parameter representing the influence of cracks is crack density, rather than porosity. For an isotropic material this parameter is defined as $e=N\langle a^3\rangle$, where N is the number of cracks per unit volume, and $\langle a\rangle$ is the mean value of the characteristic length of the cracks (O'Connell & Budiansky 1974).

Figure 7 presents the variations, according to the SC model, of the longitudinal velocity with porosity (from pores) for materials containing pores and a constant value of the crack density. In this case porosity due to microcracks is negligible, but the effect they have on the dynamic properties is noticeable. It can be observed that a good hypothesis could be to assume that the calcarenite is affected by crack densities which increase proportionally with porosity.

The presence of cracks in the calcarenite can also be suggested by the increase in velocities observed in the initial phase of isotropic or uniaxial compression tests. In fact, the longitudinal velocity of the rock specimens utilized for these tests varies between 3.00-3.25 km/s (V_P/V_{Pm} = 0.46-0.50); as shown in Figure 7 the SC model would require a crack density of 0.25 to justify these values. However, as will be discussed later, during the initial phase of the isotropic tests, P-wave velocity increases up to a maximum value of 3.55 km/s (at a stress of about 10 MPa), leading to an estimate of only 0.05 of closed crack density at this pressure. This amount of crack density appears to be too low with respect to the prediction of the models, even though the structure of the rock under load may have collapsed before all cracks had closed.

4.2 *Saturated conditions*

The influence of saturation on wave velocities depends on the relative importance of two factors acting in opposite directions: increase in moduli in undrained conditions and increase in volumic mass. According to the MT and DSC models, saturation causes a decrease in velocities when only pores are present and an increase in the case of cracks. The situation is more complex when other theoretical models are adopted or when the rock contains both cracks and pores.

During the transit of a wave, in the hydraulic condition that corresponds to an *equilibrated* pore pressure in all the voids contained in a representative element of volume (REV), the undrained bulk and shear moduli of the rock, K_u and G_u, are related to those of the dry condition, K_d and G_d, by the well known Gassmann relationships (Gassman 1951; Biot 1956), which do not depend on the structure of the voids

$$G_u = G_d$$
$$C_u = C_d - \frac{(C_d - C_m)^2}{(C_w - C_m)\phi + (C_d - C_m)} \quad (1)$$

where C is the bulk compressibility (indexes 'm' and 'w' indicate intact material and water).

However at high values of wave frequency, and therefore possibly at ultrasonic frequencies, the voids behave as *isolated* entities having different fluid pressure values. This condition leads to higher values of the undrained moduli than those predicted by the rel. (1) if microcracks are present.

Figure 4 shows the trend predicted by the Gassmann relationships and the trend obtained by assuming that saturation does not modify the moduli of the rock. The ultrasonic velocities of fully saturated specimens measured in laboratory are above the Gassmann curve because cracks and pores behave (at least in part) as isolated entities. Instead the velocities measured in situ on the calcarenite are in agreement with the Gassmann relationships; this is probably due to the low seismic frequencies adopted in these tests. Laboratory specimens in which only the free porosity is saturated are characterized by velocities in agreement with the values calculated on the basis of dry moduli and which account for the presence of water (S_t = 0.70). In this saturation condition the rock behaves as if the voids were saturated by a fluid having very high compressibility determined by the relative proportions of water and air.

Finally, the increase in the P-wave velocity observed during the drainage test when S_c decreases from 1.00 to 0.85 (Fig. 5) is probably due to the escape of water from the larger voids of higher aspect ratio, which reduces density but only slightly affects the stiffness of the rock.

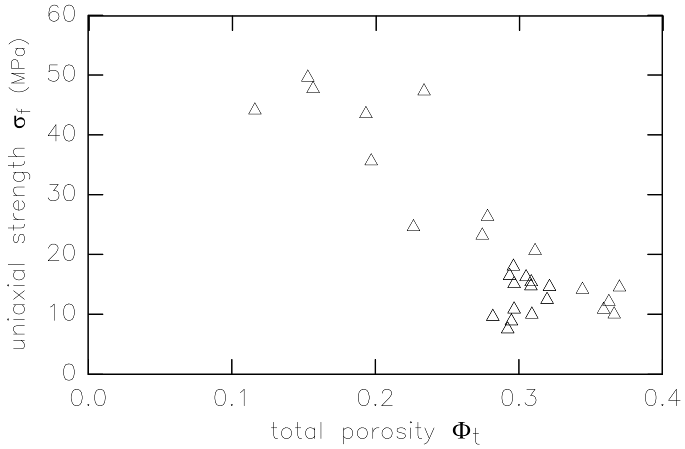

Figure 8. Uniaxial compression strength vs. total porosity.

5 STRENGTH CHARACTERISTICS

The uniaxial strength of the calcarenite, including the results from Borsetto et al. (1994), correlates well with porosity (Fig. 8), even if according to a linear regression the scatter is quite large with a standard deviation of the estimated value of 6.8 MPa, as was observed also in other soft rocks (Aversa & Evangelista 1997).

The calcarenite behaves typically like a highly porous rock, whose structure collapses at a critical value of the isotropic stress. The strength criterion was determined by means of a large number of triaxial tests, performed on specimens (in equilibrium with the laboratory conditions) having a porosity in the range 0.28-0.32. In Figure 9 the strength criterion is shown in terms of σ_1 versus σ_3; in isotropic stress conditions the strength corresponds to the yield stress, taken from the sharp elbow of the mean stress-volumetric strain curve.

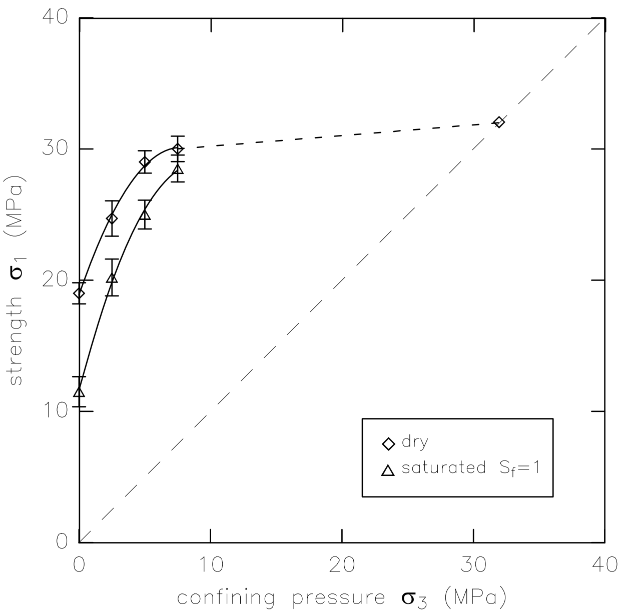

Figure 9. Mean values and standard deviations (for each confining pressure) of the triaxial strength σ_1 vs. the confining pressure σ_3 for dry and saturated specimens.

The trend of σ_1 versus σ_3 shows an initial increase, which can be interpreted by means of an equivalent friction angle of about 29° (at low values of the confining stress), followed by a plateau (or a very slow gradient) when σ_1 reaches values close to those of the yield stress in isotropic stress conditions.

For specimens saturated at S_f = 1.0 (only free porosity was saturated) the slope of the strength curve is similar, but the strength values are markedly lower (Fig. 9). This behaviour has been attributed by some Authors to frame weakening in the presence of adsorbed water. However, another hypothesis may be made on the basis of the results obtained by Papamichos et al. (1997); tests carried out in specimens of artificial sandstone at equilibrium with different values of vapour pressure have shown an increase in strength (and also in volumetric stiffness in the elastic phase) at decreasing values of water saturation. This behaviour is caused by the strong suction by capillary forces and could explain the increase in strength measured in the calcarenite on the uncompletely dry specimens (at the conditions of ambient moisture).

6 MECHANICAL TESTS

To investigate the mechanical behaviour of the calcarenite, loading tests on cylindrical specimens (54 mm in diameter and with a height-to-diameter ratio of 2) were performed. All the tested specimens had a porosity ranging between 0.28 and 0.32.

The tests were carried out at a constant axial displacement rate of 0.145 mm/min utilizing an electric motor drive unit, having a stiffness of 50 kN/mm. In the triaxial tests a conventional Hoek cell, especially suited for rock, was utilized. Both the axial and transversal deformations were measured through two pairs of strain gauges (20 mm in height). Also the external axial displacements were measured by means of a pair of extensometers located at 1/4 and 3/4 of the specimen height in the uniaxial tests and between the loading steel platens in the triaxial tests.

During some of the isotropic triaxial tests a series of small unloading-reloading cycles (0.5-1.0 MPa) of the axial load, at constant lateral stress, were performed.

Compressional and shear wave velocities in the axial direction were determined by means of the Pundit impulse generator, in which P- and S-wave transducers (300-800 kHz frequency) are mounted inside the platens of a conventional Hoek cell. No acoustic couplant was interposed between the specimen and the platens.

In uniaxial tests P- and S-wave velocities were determined also in the transversal direction by means of two pairs of Panametrics transducers (15 mm in diameter and 1 MHz in frequency), glued to flattened portions of the lateral surface of the specimens.

Waveforms and data relative to the static measurements were acquired and stored through two PCs. The use of a common time base has allowed to merge the data.

Wave attenuation variations during the tests were qualitatively estimated on the basis of the maximum wave amplitude; it should be taken into account that, for the dynamic measurements in the axial direction, this parameter is influenced also by the joints between the platens and the specimen.

6.1 *Isotropic triaxial tests*

Figure 10 shows typical curves obtained from isotropic triaxial tests in calcarenite specimens. The volumetric strain (from the strain gauges) versus isotropic stress curves always show a well defined yield condition, representing the boundary between an almost elastic and a strain hardening plastic behaviour. The variability of the material's compressibility and strength is evident.

The static and dynamic behaviour of a typical specimen observed during an isotropic triaxial test (at a maximum pressure of 60 MPa) is presented in Figure 11. The related tangent static bulk modulus and the dynamic one are compared in Figure 12. During the test the following phases can be distinguished:

- OA) In the initial elastic compression phase, that is to say up to 50-70% of the yield stress, there is a slight velocity increase (about 10%) and a marked increase in wave amplitudes. In the Figures 11 and 12 point A corresponds to the maximum value of the P-wave velocity. For this specimen the static modulus increases up to a higher value than the dynamic one, but this behaviour does not apply in general.
- ABC) The yield (point B) and the subsequent large plastic strains do not markedly influence the wave velocities and the dynamic elastic constants. Instead at yield the bulk deformation modulus sharply decreases to about 5 % of the maximum value in the pre-yield phase.
- CD) The stress-strain curve is almost linear up to a relatively large strain. A larger decrease in wave velocities and in wave amplitudes is observed.
- DE) In the final loading phase the static curve shows a slight steepening, that is an increase in the hardening modulus. Even the dynamic characteristics show a slight increase, whereas amplitudes variations are much larger.
- EF) At unloading, the stress-strain curve is markedly concave upwards, especially at the lower stresses. Velocities initially remain at the same level as in the loading phase, but afterwards they decrease markedly. The final dynamic modulus of the unloaded specimen is about 25% of the initial value.

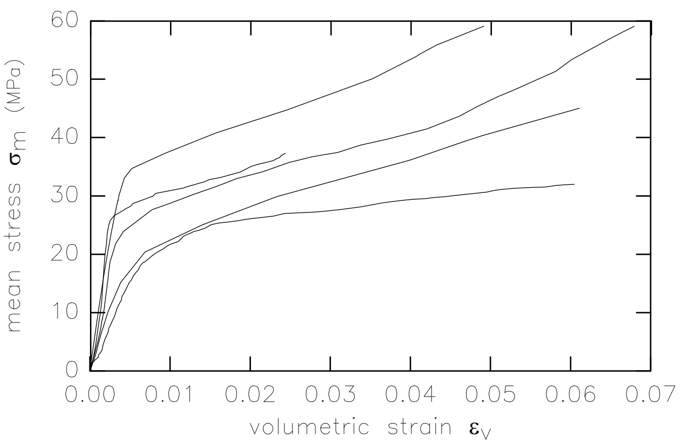

Figure 10. Curves of mean stress vs. volumetric strain obtained during triaxial isotropic tests.

According to some Authors (Addis 1989, Powell & Lovell 1994, Scott et al. 1995), after the elastic phase the compaction of the rock is produced by pore collapse, which brings about grain displacement, breaking of the cement bond, fracturing of the grains and twinning of the calcite grains. The behaviour of the calcarenite can be explained by assuming that after yield, two contrastating effects are at work, a void reduction which produces a higher number of grain contacts as well as an increase in both strength and volumetric stiffness, and a breaking of the intergranular bonds which causes a decrease in both strength and volumetric stiffness. The increase in the hardening modulus and in the dynamic characteristics observed in the calcarenite during the last phase (DE) is probably related to the prevailing effect of the former factor. The interaction of these two factors brings about different mechanical behaviours and varies with the texture of the rock; e.g. for a soft calcarenite a strain softening phase has been observed after yield, followed by a steady increase in the hardening modulus (Lagioia & Nova 1995).

The low values of the dynamic modulus in the unloading phase indicate that plastic strains produced a loss of structure (Leroueil & Vaughan 1990) of the calcarenite.

For this test, the Young modulus was estimated from the static measurements during the small unloading-reloading cycles. Static and dynamic Young moduli, measured in the elastic phase (0-12 MPa), are compared in Figure 13 with respect to axial stress. The static modulus is always lower than the dynamic modulus, even if it slightly tends to come closer to the dynamic one, as was also determined on a sandstone by Hilbert et al. 1994.

6.2 *Uniaxial compression tests*

In uniaxial stress conditions the calcarenite behaves like a brittle and dilatant material (Fig. 14); because of the lesser value of machine stiffness respect with

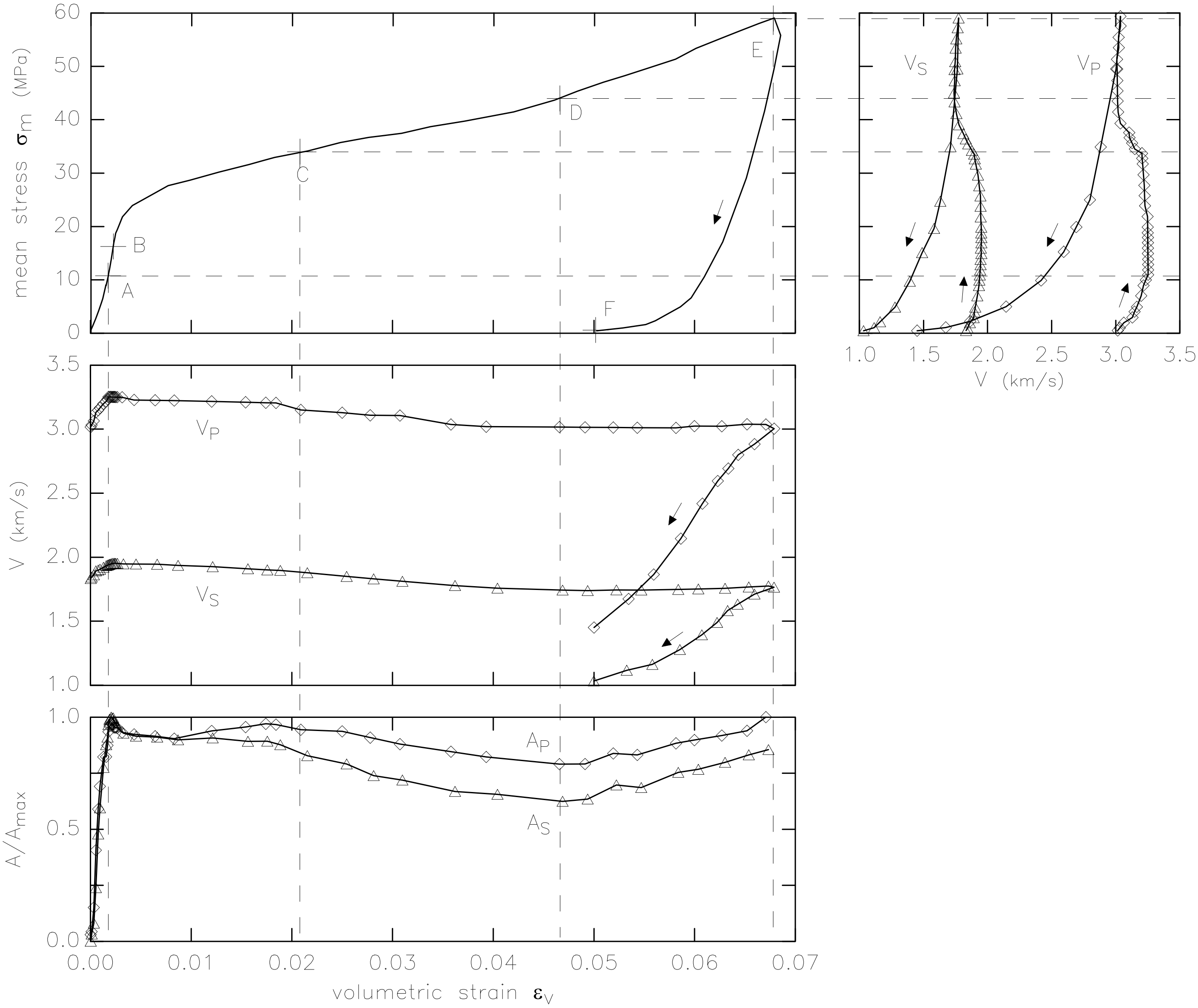

Figure 11. Curve of mean stress vs. volumetric strain (top) obtained during a triaxial isotropic test. Corresponding curves of P- and S-wave velocities and normalized wave amplitudes vs. volumetric strain are shown below; corresponding curves of P- and S-wave velocities vs. mean stress are shown on the right.

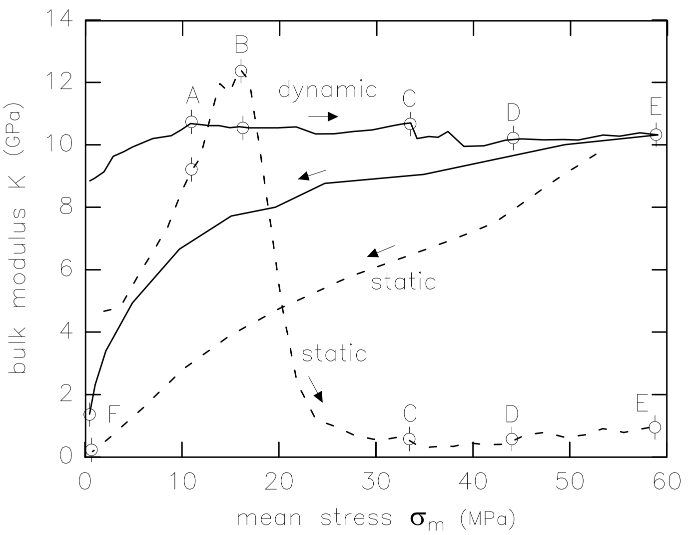

Figure 12. Bulk moduli from static and dynamic measurements obtained from the same test as Figure 11 during a triaxial isotropic test.

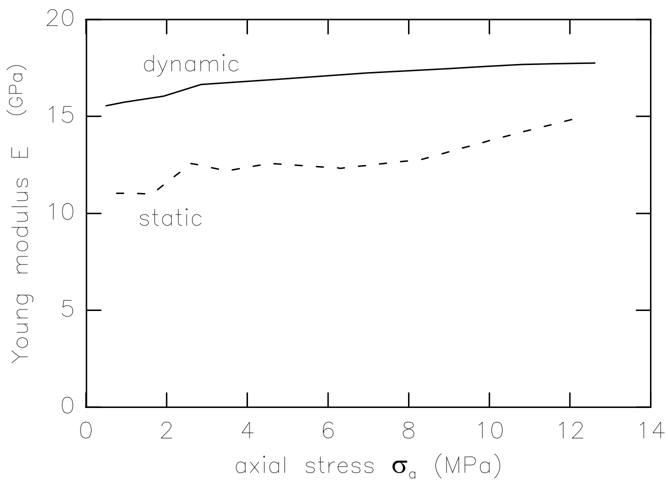

Figure 13. Elastic Young moduli from static and dynamic measurements obtained from the same test as Figure 11 during a triaxial isotropic test. The static modulus has been determined from unloading cycles of the axial stress.

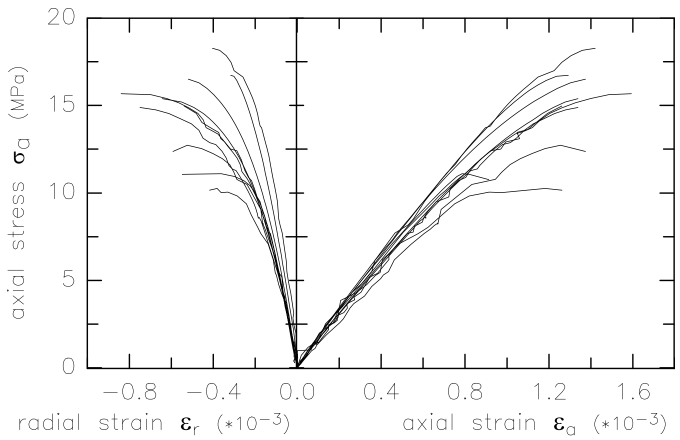

Figure 14. Curves of axial stress vs. strains obtained during uniaxial compression tests.

to specimen stiffness (50 kN/mm against 250 kN/mm), when failure occurs, the amount of energy stored in the testing machine is released onto the specimens, resulting in abrupt rupture (Jaeger & Cook 1969).

The detailed results obtained for a typical specimen are shown in Figure 15. The trends of the wave velocities in the axial direction 1 and in the transversal direction 3 indicate a stress-induced anisotropy of the specimen. In the initial loading phase (up to about 2/3 of the failure stress) the increase in the axial longitudinal velocity (V_P^1) and, to a lesser extent, in the shear velocity (V_S^{13}) is probably due to the closing of microcracks, in particular those which are orientated normally to the applied stress; the closure does not influence the velocities in the transversal direction (V_P^3 and V_S^{23}). At higher stresses, dilatancy occurs gradually; this is likely to be caused by the development of subaxial cracks which affect the velocities and the wave amplitudes much more in the transversal direction than in the axial direction. The trends of the wave amplitudes with stress are in agreement with the microcrack development model that has been suggested, and which is very similar to what occurs in hard brittle rocks. It is to be noted that the steady

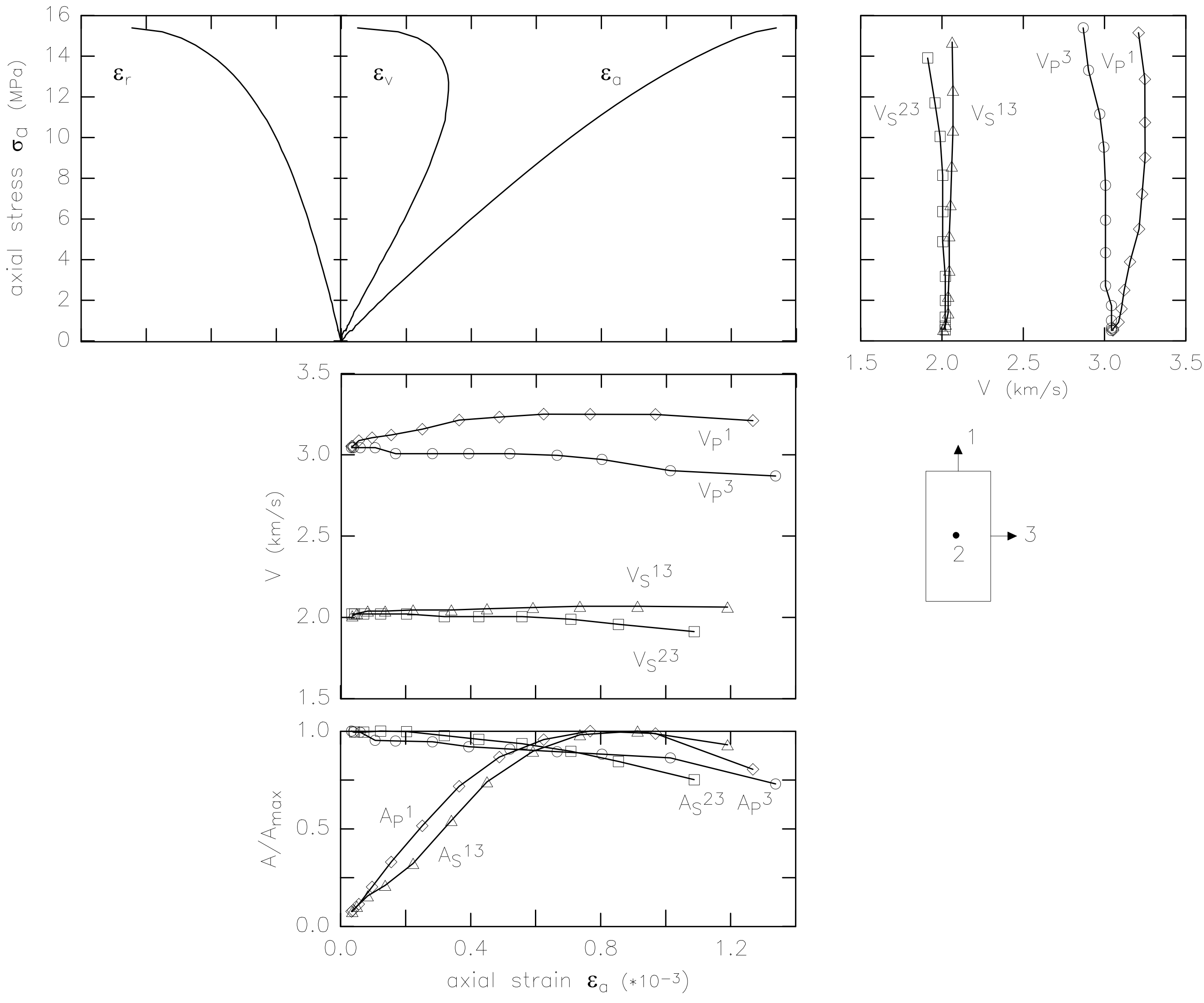

Figure 15. Curves of axial stress vs. strains (top) obtained during a uniaxial compression test. Corresponding curves of P- and S-wave velocities and normalized wave amplitudes vs. axial strain are shown below; corresponding curves of P- and S-wave velocities vs. axial stress are shown on the right.

decrease of the maximum wave amplitudes measured in the transversal direction possibly indicate the formation of new cracks even at low values of the stress.

The Young dynamic moduli (E_1 and E_3), which have been evaluated from the measured velocities on the basis of a first order approximation (that is with the same relationships which are adopted for an isotropic medium), are displayed, together with the static Young modulus E_1, in Figure 16. At low stress levels of deformation the moduli have similar values, but at higher stresses the differences increase, evidencing that anelastic strains (which can be due to a sliding of closed cracks or to the local crushing of bonds) occur long before failure. However, in comparison with the behaviour of other soft rocks having a high clay content (mudstones and shales) (Tatsuoka et al. 1993), the degradation of the static moduli with respect to the initial values is much less important for stress levels close to failure.

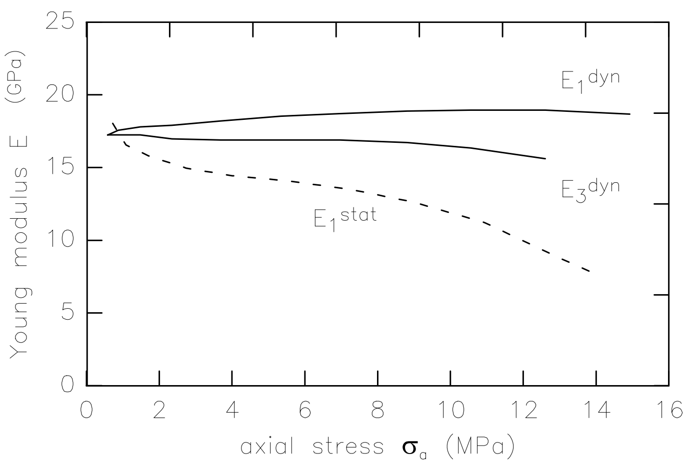

Figure 16. Elastic Young moduli from static (E_1) and dynamic measurements (E_1 and E_3) obtained from the same test as Figure 15 during a uniaxial compression test.

7 CONCLUSIONS

The textural characteristics have a marked influence on the mechanical behaviour of the calcarenite, as shown by the strong variability of the strength and elastic parameters for specimens having similar porosity. The textural characteristics for this type of rock are related to deposition conditions and do not appear to be markedly influenced by the lithostatic load.

Wave velocities appear to be a very sensitive index of the texture variations both in unstressed conditions and during loading. The correspondence between seismic velocities and wave amplitude suggests that they are controlled by the same mechanism, as was indicated by other Authors (Ita et al. 1993). Moreover wave amplitude, even though it is a qualitative index, has been evidenced to be more sensitive than velocity in indicating variations in the textural characteristics of the rock during loading tests.

The elastic constants of the material before the yield and during the hardening phase can be determined from the wave velocities in a more simple and reliable way than is usually done by means of small static unloading cycles.

For this type of rock the elastic moduli in isotropic stress conditions show a small increase in the elastic phase and are only slightly affected by the yield and by the subsequent large plastic deformations in the hardening phase.

In uniaxial stress conditions the measurements in axial and transversal directions evidence a stress-induced anisotropy, related to the closing of pre-existing cracks and to the subsequent damage caused by the opening up of new cracks.

ACKNOWLEDGEMENTS

The author would like to thank Professor Renato Ribacchi for his encouragement and useful suggestions. Also the contribution of the anonymous referee has been greatly useful in improving the discussion.

The author kindly acknowledges the University of Tor Vergata, Rome, where the mercury porosimeter tests were carried out.

This research was partially carried out with the financial support of MURST (Ministero dell'Università e della Ricerca Scientifica).

REFERENCES

Addis, M.A. 1989. The behaviour and modelling of weak rocks. In Maury & Fourmaintraux (eds), *Proc. Int. Conf. Rock at Great Depth, Pau*: 899-905. Rotterdam: Balkema.

Aversa, S. & A. Evangelista 1997. The mechanical behaviour of a pyroclastic rock: yield strength and 'destructuration' effects. *Rock Mech. Rock Engng.* 31(1): 25-42.

Berge, P.A., B.P. Bonner & J.G. Berryman 1995. Ultrasonic velocity-porosity relationships for sandstone analogs made from fused glass beads. *Geophysics*. 60(1): 108-119.

Biot, M.A. 1956. Theory of propagation of elastic waves in a fluid-saturated porous solid. I. Low-frequency range. II. Higher frequency range. *J. Acoust. Soc. Am.* 28: 168-191.

Blangy, J.P., S. Strandenes, D. Moos & A. Nur 1993. Ultrasonic velocities in sands- revisited. *Geophysics*. 58(3): 344-356.

Borsetto, M., A. Frassoni, P.P. Rossi, C. Garbin & T. Moro 1984. The Anapo pumped-storage power station: geomechanical investigations and design criteria. *Proc. ISRM/BGS Symp. Design and Performance of underground excavations, Cambridge*: 73-80.

Bourbie, T. & B. Zinszner 1985. Hydraulic and acoustic properties as a function of porosity in Fontainebleau sandstone. *J. Geoph. Res*. 90(B13): 11524-11532.

Cleary, M.P., I. Chen & S. Lee 1980. Self-consistent techniques for heterogeneous media. *J. Eng. Mech. Div*. 106: 861-887.

Gassmann, F. 1951. Über die elastizität poröser medien. *Mitteilungen aus dem Inst. Geoph*., 17: 1-23.

Han, D., A. Nur & F.D. Morgan 1986. Effects of porosity and clay content on wave velocities in sandstones. *Geophysics*. 51(11): 2093-2107.

Hilbert, Jr. L.B., T.K. Hwong, N.G.W. Cook, K.T. Nihei & L.R. Myer 1994. Effects of strain amplitude on the static and dynamic non-linear deformation of Berea sandstone. *Proc. 1st North Amer. Rock Mech. Symp., Austin*: 497-504.

Knight, R. & R. Nolen-Hoeksema 1990. A laboratory study of the dependence of elastic wave velocities on pore scale fluid distribution. *Gephys. Res. Lett*. 17: 1529-1532.

Kuster, G.T. & N.M. Toksoz 1974. Velocity and attenuation of seismic waves in two-phase media: Part I. Theoretical formulations. Part II. Experimental results. *Geophysics.* 39: 587-618.

Ita, S.L., N.G.W. Cook, L.R. Myer & K.T. Nihei 1993. Effects of stress anisotropy on the static and dynamic properties of Berea sandstone. *Int. J. Rock Mech. Min. Sci*. 30(7): 785-788.

Jaeger, J.C. & N.G.W. Cook 1969. Fundamentals of rock mechanics. London: Chapman and Hall.

Lagioia, R. & R. Nova 1995. An experimental and theoretical study of the behaviour of a calcarenite in triaxial compression. *Géotechnique.* 45(4): 33-648.

Leroueil, S. & P.R. Vaughan 1990. The general and congruent effects of structure in natural soils and weak rocks. *Géotechnique*. 40(3): 67-488.

Mori, T. & K. Tanaka 1973. Average stress in matrix and average elastic energy of materials with misfitting inclusions. *Acta Metallica*. 21: 571-574.

Murphy, W.F. III 1984. Acoustic measures of partial gas saturation in tight sandstones. *J. Geoph. Res*. 89(B13): 11549-11559.

O'Connell, R.J. & B. Budiansky 1974. Seismic velocities in dry and saturated cracked solids. *J. Geoph. Res*. 79: 5412-5426.

Papamichos, E., M. Brignoli & F.J. Santarelli 1997. An experimental and theoretical study of a partially saturated collapsible rock. *Mech. Cohes.-Frict. Mater.* 2: 251-278.

Powell, B.N. & G.L. Lovell 1994. Mechanisms of chalk compaction. *Proc. Int. Conf. SPE/ISRM Eurock '94, Delft*: 811-818. Rotterdam: Balkema.

Sayers, C.M., J.G. Van Munster & M.S. King 1990. Stress-induced ultrasonic anisotropy in Berea sandstone. *Int. J. Rock Mech. Min. Sci*. 27: 429-436.

Scott, Jr. T.E., Q. Ma & J.-C. Roegiers 1993. Acoustic velocity changes during shear enhanced compaction of sandstone. *Int. J. Rock Mech .Min. Sci*. 30: 763-769.

Scott, Jr. T.E., M. Azeemuddin, M. Zaman & J.-C. Roegiers 1995. Changes in acoustic velocity during pore collapse of rocks. *News J. ISRM*. 3(1): 14-17.

Tatsuoka, F., Y. Kohata, K. Mizumoto, Y.-S. Kim, K. Ochi & D. Shi 1993. Measuring small strain stiffness of soft rocks. *Proc. Int. Symp. Geotechnical Engineering of Hard Soils-Soft Rocks, Athens*: 809-816.

Walsh, J.B. 1965. The effect of cracks on the compressibility of rock. *J. Geoph. Res*., 70: 381-389.

Wu, B., M.S. King & J.A. Hudson 1991. Stress-induced ultrasonic wave velocity anisotropy in a sandstone. *Int. J. Rock Mech. Min. Sci*. 28: 101-107.

Zamora, M. & J.P. Poirier 1990. Experimental study of acoustic anisotrpy and birefringence in dry and saturated Fontainebleau sandstone. *Geophysics.* 55(11): 1455-1465.

Zimmerman, R.W. 1991. Elastic moduli of a solid containing spherical inclusions. *Mech. of Materials*. 12: 17-24.